Identification of a novel, widespread, and functionally important PCNA-binding motif

Karin M. Gilljam, Emadoldin Feyzi, Per A. Aas, Mirta M.L. Sousa, Rebekka Müller, Cathrine B. Vågbø, Tara C. Catterall, Nina B. Liabakk, Geir Slupphaug, Finn Drabløs, Hans E. Krokan, and Marit Otterlei

Department of Cancer Research and Molecular Medicine, Faculty of Medicine, Norwegian University of Science and Technology, N-7489 Trondheim, Norway

Numerous proteins, many essential for the DNA replication machinery, interact with proliferating cell nuclear antigen (PCNA) through the PCNA-interacting peptide (PIP) sequence called the PIP box. We have previously shown that the oxidative demethylase human AlkB homologue 2 (hABH2) colocalizes with PCNA in replication foci. In this study, we show that hABH2 interacts with a posttranslationally modified PCNA via a novel PCNA-interacting motif, which we term AlkB homologue 2 PCNA-interacting motif (APIM). We identify APIM in >200 other proteins involved in DNA maintenance, transcription, and cell cycle regulation, and verify a functional APIM in five of these. Expression of an APIM peptide increases the cellular sensitivity to several cytostatic agents not accounted for by perturbing only the hABH2–PCNA interaction. Thus, APIM is likely to mediate PCNA binding in many proteins involved in DNA repair and cell cycle control during genotoxic stress.

Introduction

Proliferating cell nuclear antigen (PCNA) is a member of the conserved sliding clamp family of proteins. It is essential for chromosomal DNA replication and important for several DNA transactions, such as DNA repair, epigenetic modification, chromatin assembly and remodeling, sister chromatid cohesion, and cell cycle control (Moldovan et al., 2007). Numerous proteins involved in these processes are localized in so-called replication factories, and many of these proteins interact with PCNA through the conserved sequence called the PCNA-interacting peptide (PIP) box (QxxL/I/MxxHF/DF/Y; Warbrick, 2000). However, several PCNA-binding proteins do not contain a PIP box (Fan et al., 2004; Moldovan et al., 2007). Furthermore, posttranslational modifications (PTMs) of PCNA have been reported to regulate the affinity to its binding partners, as illustrated by polymerase switch (Lehmann et al., 2007).

Human cells are exposed to alkylating compounds produced endogenously from environmental sources and drugs used in cancer treatment (Drabløs et al., 2004). Proteins involved in DNA repair and cell cycle control are interesting targets to increase the efficacy of chemotherapy (Helleday et al., 2008). The DNA damage introduced, such as alkylation adducts and interstrand cross-links, may lead to miscoding, replication arrest, double-strand breaks, and/or cell death. The simpler lesions, such as methylated bases, are repaired by base excision repair (BER), oxidative demethylation, or methyl transfer, depending on the type of damage (Sedgwick et al., 2007). The BER enzyme 3-methyladenine DNA glycosylase (AAG/MPG; removes 3meA) and the oxidative demethylase human AlkB homologue 2 (hABH2; repairs 1meA and 3meC) are both localized in proximity of replication foci (Aas et al., 2003; Xia et al., 2005). Although MPG contains an "inverted" PIP box sequence for interaction with PCNA, no PIP box is found in hABH2.

In this study, we demonstrate that hABH2 interacts with PCNA through a novel PCNA-interacting motif, AlkB homologue 2 PCNA-interacting motif (APIM), and that APIM is a functional PCNA-binding motif important for several proteins involved in DNA maintenance and cell cycle regulation after DNA damage.

K.M. Gilljam, E. Feyzi, and P.A. Aas contributed equally to this paper.

Correspondence to Marit Otterlei: marit.otterlei@ntnu.no

Abbreviations used in this paper: APIM, AlkB homologue 2 PCNA-interacting motif; BER, base excision repair; FRET, fluorescence resonance energy transfer; hABH2, human AlkB homologue 2; HcRed, *Hereactis crispa* RFP; IP, immunoprecipitation; LC, liquid chromatography; MMC, mitomycin C; MMS, methyl methanesulfonate; MS, mass spectrometry; PCNA, proliferating cell nuclear antigen; PCV, packed cell volume; pI, isoelectric point; PIP, PCNA-interacting peptide; PTM, posttranslational modification; TMZ, temozolomide; Topo, topoisomerase; WB, Western blot; WT, wild type.

The Rockefeller University Press $30.00
J. Cell Biol. Vol. 186 No. 5 645–654
www.jcb.org/cgi/doi/10.1083/jcb.200903138

Results and discussion

The 10 N-terminal amino acids in hABH2 are essential for colocalization with PCNA

To identify the region in hABH2 responsible for localization in replication foci during S phase (Aas et al., 2003), we coexpressed PCNA tagged with a blue variant of GFP (CFP-PCNA) and various hABH2 deletion mutants fused with a yellow GFP variant (YFP) because GFP-tagged PCNA is known to form foci representing sites of replication (Leonhardt et al., 2000). First, we verified that hABH2-YFP colocalized with endogenous PCNA similar to coexpressed, tagged PCNA (Fig. 1 A, rows 1 and 2). Next, we found that deletion of the 10 N-terminal amino acids in hABH2 totally abolished the colocalization with PCNA. Remarkably, these 10 amino acids fused to YFP were sufficient for colocalization with PCNA (Fig. 1 A, rows 3 and 4). Notably, coexpression of CFP-PCNA increased the localization of full-length hABH2 ($hABH2_{1–261}$-YFP) but not $hABH2_{11–261}$-YFP in nuclear foci, suggesting a direct interaction between PCNA and hABH2 mediated by the 10 N-terminal amino acids of hABH2.

To investigate the potential hABH2–PCNA interaction in more detail, soluble and chromatin-enriched protein extracts were prepared from cells expressing hABH2-YFP, $hABH2_{11–261}$-YFP, or YFP and subjected to coimmunoprecipitation (co-IP) using anti-YFP antibodies (α-YFP). Notably, low levels of PCNA were pulled down from the soluble cell fraction, whereas PCNA was readily pulled down from the chromatin-enriched fraction. Moreover, removal of the 10 N-terminal residues in hABH2 markedly decreased the amount of PCNA pulled down (Fig. 1 B). The hABH2–PCNA interaction was confirmed by reciprocal experiments using extracts from cells expressing YFP-PCNA (Fig. 1 C) and also by targeting endogenous PCNA (Fig. 1 D). In both cases, more hABH2 was pulled down from the chromatin-enriched fractions than from the soluble fractions (Fig. 1, C and D), even though both proteins were present in the soluble fraction (Fig. 1 D, input). Collectively, these results support the idea that hABH2 interacts with PCNA and that the binding sequence is contained within hABH2's 10 N-terminal amino acids. The apparent preferential association of hABH2 and PCNA in the chromatin-enriched fraction may indicate that a subfraction of either of the proteins exists in a PTM form, promoting the interaction. Alternatively, the presence of other proteins may mediate the observed interaction. A bridging effect caused by DNA interaction was considered less likely because the chromatin-enriched fraction was subjected to extensive DNase and RNase treatment before co-IP.

hABH2 directly interacts with PCNA through a novel PCNA-binding motif

Sequence alignment of ABH2s from several species shows that the seven N-terminal amino acids are highly conserved (Fig. 2 A) and have the apparent consensus Met-Asp-Lys/Arg-Phe-$(Leu/Val/Ile)_2$-Lys/Arg. The flanking amino acids (8–10) are not conserved. Dot blot assays against mutant versions of this sequence indicated that the most important determinant for binding to PCNA was an aromatic residue at position 4 because Tyr could substitute for Phe at this position, whereas Ala abolished the interaction (Fig. 2 B and not depicted). We verified the sequence specificity for the PCNA interaction in vivo by expressing the conserved amino acids 1–7 of hABH2, and variants in which Phe4 was substituted by Tyr, Trp, or Ala, in fusion with YFP and tested their subnuclear localization. Expressed fusion proteins containing an aromatic amino acid in position 4 colocalized with PCNA when expressed alone (Fig. 2 C, rows 1 and 2) and when coexpressed with CFP-PCNA (Fig. 2 C, rows 3–5). Analogous to what was found in dot blot assays, the F4A mutation severely reduced the colocalization with PCNA (Fig. 2 C, row 6). By measuring fluorescence resonance energy transfer (FRET), we found that both full-length hABH2-YFP and $hABH2_{1–10}$-YFP as well as $hABH2_{1–7}$F4W-YFP are in very close proximity with CFP-PCNA because fluorescent tags must be <100 Å apart to give positive FRET (Mátyus, 1992).

To further investigate the proximity between hABH2 and PCNA, we performed in vivo cross-linking in cells stably expressing $hABH2_{1–7}$-YFP-Flag and $hABH2_{1–7}$F4A-YFP-Flag using formaldehyde. Formaldehyde induces heat-reversible cross-links of proteins that are within ∼2 Å of one another (Vasilescu et al., 2004). Extracts from these cells were used for IP with α-Flag. After elution with Flag peptide, cross-links in half of the samples were reversed. In Fig. 2 E (lanes 3 and 11), bands containing both PCNA and Flag are identified at molecular masses of ∼70–75 kD (1: PCNA cross-linked to $hABH2_{1–7}$-YFP-Flag), 100–130 kD (2: PCNA dimer or trimer cross-linked to $hABH2_{1–7}$-YFP-Flag), and 160–190 kD (3: PCNA trimer cross-linked to two or three $hABH2_{1–7}$-YFP-Flag). Bands 1 and 2 are much stronger in the IP from cells expressing $hABH2_{1–7}$ wild type (WT) than from cells expressing the $hABH2_{1–7}$F4A mutant, and band 3 is not detected in the IP from cells expressing the $hABH2_{1–7}$F4A mutant. Notably, after reversal of the cross-links (lanes 4 and 12), only PCNA and Flag bands of 35 kD were identified, suggesting that the larger bands detected in lanes 3 and 11 were cross-linked with $hABH2_{1–7}$-YFP-Flag and PCNA. Together with the FRET, these data strongly support a direct interaction between $hABH2_{1–7}$ and PCNA.

Our data from co-IP experiments (Fig. 1, B–D) indicated that more complexes of hABH2 and PCNA were pulled down from chromatin-enriched fractions, suggesting potential involvement of PTMs. Therefore, we analyzed the isoform distribution of PCNA cross-linked to $hABH2_{1–7}$-YFP-Flag by 2D Western blot (WB) analysis and compared it with the total repertoire of PCNA isoforms present in the same cell extract (Fig. 2 F). We included purified RAD51 as an internal standard because its isoelectric point (pI; 5.4) is close to the pI of unmodified PCNA (4.6). Our results indicate that the PCNA variants cross-linked to $hABH2_{1–7}$-YFP-Flag (top membrane) are shifted toward a more acidic pI without significantly changing the vertical migration. Multiple isoforms of PCNA with pI between 4 and 5 have previously been identified, although the exact nature of most of these modifications is not known (Naryzhny, 2008). Most PCNA present in a cell (lower membrane), and the low levels (Fig. 2 E, lane 7) of PCNA cross-linked to $hABH2_{1–7}$F4A-YFP-Flag (mutant; mid membrane), have a higher pI than the PCNA pulled down by

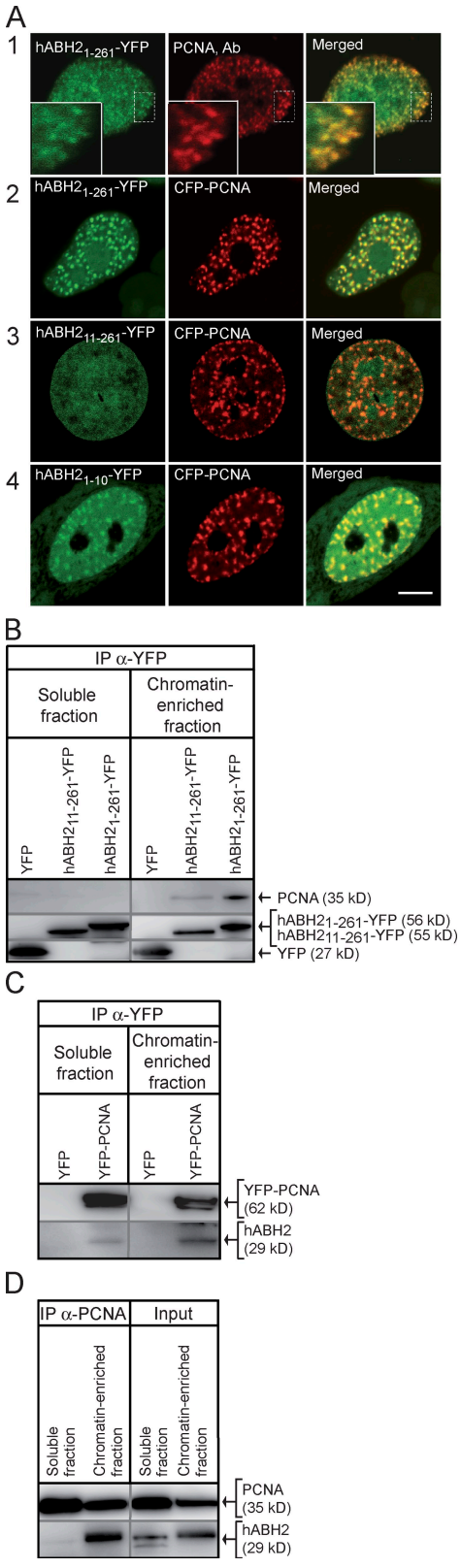

Figure 1. **The 10 N-terminal amino acids of hABH2 are important for interaction with PCNA.** (A) Confocal fluorescence images of full-length hABH2-YFP with endogenous PCNA (row 1) and hABH2 constructs co-expressed with CFP-PCNA in live cycling HeLa cells. Insets show a higher magnification view of boxed regions. Bar, 5 µm. (B) Co-IP of PCNA from HeLa cells stably expressing hABH2-YFP constructs using α-YFP beads. (C) Co-IP of hABH2 from cells stably expressing YFP-PCNA using α-YFP beads. (D) Co-IP of hABH2 from cells only expressing endogenous proteins using α-PCNA beads. Input is 3.3% of cell extract used for IP. Black lines, separate membranes; gray lines, same membranes.

hABH2$_{1–7}$-YFP-Flag. PTMs on PCNA may explain why our attempts to analyze the PCNA–hABH2 interactions using purified recombinant full-length proteins in in vitro experiments gave inconclusive data.

Collectively, these results reveal a novel PCNA-binding site within the conserved seven N-terminal amino acids of hABH2. Based on the alignment of the different ABH2s, the dot blot assay, and the in vivo imaging results, APIM was defined as [KR]-[FYW]-[LIVA]-[LIVA]-[KR].

Overexpression of APIM decapeptide fused to YFP reduces repair of 1meA and sensitizes cells to DNA alkylation damage

hABH2 is known to repair 1meA and 3meC generated by the S_N2-alkylating agent methyl methanesulfonate (MMS) (Aas et al., 2003; Ringvoll et al., 2006). To examine whether expression of APIM interfered with the function of hABH2 by perturbation of the PCNA binding, we exposed cells expressing hABH2$_{1–10}$-YFP or only YFP to MMS and analyzed removal of 1meA in DNA by liquid chromatography (LC)/mass spectrometry (MS)/MS. Cells were arrested at the G1/S border and treated with MMS for 1 h. For arrested cells, a 13% significant increase of 1meA was seen in APIM-YFP–expressing compared with YFP-expressing cells (Fig. 3 A). This is likely the result of reduced removal of 1meA by endogenous hABH2 during incubation with MMS. These results indicate that the hABH2–PCNA interaction is required for efficient removal of 1meA in cells arrested at the G1/ S transition.

Next, we exposed cell lines expressing hABH2$_{1–10}$-YFP, hABH2$_{1–7}$F4A-YFP, and YFP to MMS and measured their colony-forming capacity. We found a fivefold decrease in colony-forming units in cells overexpressing functional hABH2$_{1–10}$-YFP compared with the cells expressing mutated APIM and only YFP (Fig. 3 B). These results strongly suggest that binding of APIM to PCNA increases MMS cytotoxicity. We subsequently exposed hABH2$_{1–10}$-YFP– and YFP-expressing cells to MMS as well as three other alkylating agents, BCNU (carmustine), temozolomide (TMZ), and mitomycin C (MMC), and measured cell growth for 4 d (MTT assay [3-(4,5-dimethylthiazol-2-yl)-2,5-diphenyltetrazolium bromide]). Unlike MMS, the other alkylating agents are believed to introduce damage not repaired by hABH2 but by several different repair pathways, including direct methyl transfer by O^6-methylguanine-DNA methyltransferase, nucleotide excision repair, BER, mismatch repair, and homologous recombination (Sedgwick et al., 2007). Over expression of hABH2$_{1–10}$-YFP had little effect on the growth rate in untreated cells, whereas it strongly sensitized cells to all the alkylating agents (Fig. 3 C). These results suggested that the hypersensitivity to genotoxic agents was caused by inhibiting the function not only of hABH2 but also of other proteins involved in genome maintenance.

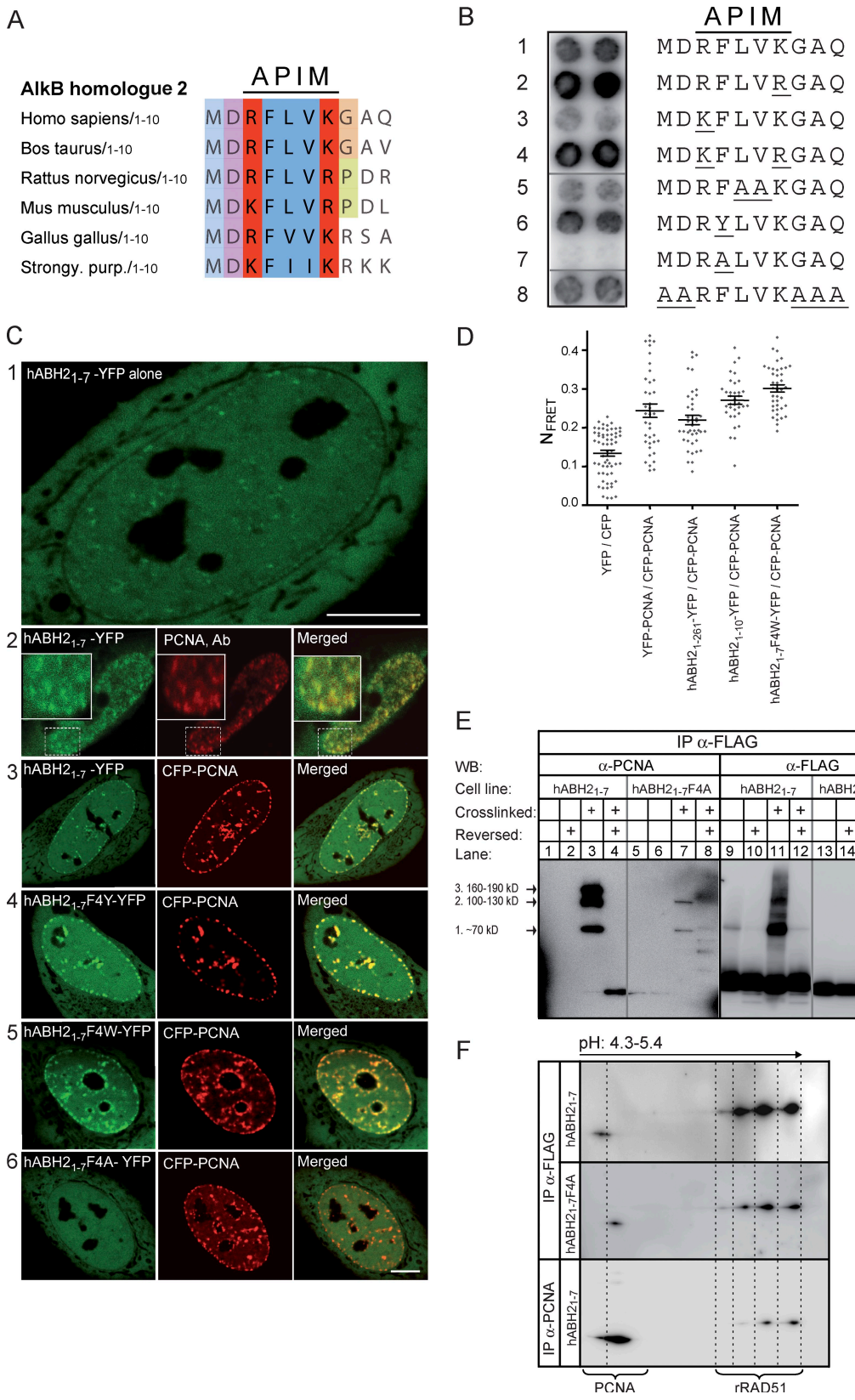

Figure 2. **Close interaction between the N terminus of hABH2 and a modified form of PCNA.** (A) Sequence alignment of the 10 N-terminal amino acids of ABH2 homologues from different species (colors as given by Clustal X). (B) PCNA binding to hABH2$_{1-10}$ peptide variants (dot blot). Row 1 shows the hABH2$_{1-10}$ peptide, and rows 2–8 show peptides where different amino acids are substituted (underlined in the right panel; data from one membrane). (C) Confocal images of HeLa cells. Row 1 shows hABH2$_{1-7}$-YFP expressed alone (live cells), row 2 shows hABH2$_{1-7}$-YFP with endogenous PCNA, and rows 3–6 show various hABH2$_{1-7}$-YFP F4 variants coexpressed with CFP-PCNA (live cells). Insets show a magnified view of the boxed areas. Bars, 5 µm. (D) N$_{FRET}$ measurements. YFP/CFP (vectors only) and YFP-PCNA/CFP-PCNA were used as background and positive controls, respectively. Data shown

APIM is found in many proteins involved in genome maintenance and cell cycle control

Using the APIM motif as the query, we obtained 636 hits in the Swiss-Prot/TrEMBL database. After discarding nonnuclear proteins and proteins in which APIM is not conserved, this was reduced to 226 hits (Table I; see http://tare.medisin.ntnu.no/pcna/index.php for complete query results and experimental procedures). Nine of these proteins also contained the PIP box consensus (Table I).

Among the proteins found in the query, we examined the APIMs more closely in four human proteins in addition to hABH2. We named the first protein examined TFIIS-like (TFIIS-L) because it contains the conserved N-terminal domain I found in elongation factor TFIIS (Cramer, 2004). The function of this protein is unknown. However, like hABH2, TFIIS-L contains an APIM within its seven N-terminal amino acids. We next examined the multifunctional transcription factor TFII-I, which contains four APIMs. TFII-I is a transcription factor critical for cell cycle control and proliferation and has also recently been suggested to have a role in DNA repair (Desgranges and Roy, 2006). Finally, we examined APIM in DNA topoisomerase (Topo) II α, which is involved in postreplicative DNA decatenation and DNA segregation (Agostinho et al., 2004), and the RAD51 paralogue RAD51B, which is involved in homologous recombination, centrosome function, and chromosome segregation (Date et al., 2006). The APIM sequences in all these proteins are conserved throughout evolution (Fig. 3 D). Among these proteins, only Topo II α has been reported to localize to nuclear S phase foci (Lou et al., 2005) and to contain a putative PIP box (QttLaFkp; amino acids 1,277–1,284; Niimi et al., 2001). We cloned the proteins as YFP fusions and found that all were nuclear proteins accumulating in various numbers of visible foci (Fig. 3 D), many of which represent replication foci (see following paragraph). Endogenous TFII-I was also present in foci colocalizing with endogenous PCNA (unpublished data).

APIM is a functional PCNA-interacting motif

Substitution of Phe4 to Ala in APIM impaired binding between hABH2-derived peptides and PCNA (Fig. 2); thus, we wanted to examine whether the corresponding mutation had a similar effect on the full-length hABH2, TFIIS-L, TFII-I (in one and four APIMs), Topo II α, and RAD51B. Mutation of APIM in all these proteins, except Topo II α, strongly reduced colocalization with PCNA when coexpressed with WT proteins (Fig. 4 A, rows 2–7), suggesting that impaired APIM reduced the PCNA interaction. However, coexpression of WT hABH2-CFP and WT hABH2-YFP resulted in foci containing both fusion proteins (Fig. 4 A, row 1). Mutations of APIM in TFIIS-L, or in either one of the four APIMs of TFII-I, did not cause visible reduction in colocalization with PCNA when cotransfected with PCNA alone (unpublished data), but a reduction in FRET could be detected in these cases (Fig. 4 B, green). Thus, higher FRET between PCNA and WT proteins, and the fact that WT proteins outcompete the mutant proteins for binding to PCNA when coexpressed (Fig. 4 A, rows 3 and 4), suggested that the affinity of the mutant proteins for PCNA was reduced. Only a minor reduction in colocalization with PCNA was observed for the mutant Topo II α when coexpressed with WT Topo II α. However, a reduction in FRET was also detected in this case (Fig. 4 B). Because Topo II α is a homodimer (Nettikadan et al., 1998), binding to PCNA could be mediated through its nonmutated endogenous or coexpressed WT partner. Altogether, these results strongly suggest that APIM is a functional PCNA-binding motif in all these proteins.

The RAD51B S phase spots were on average less bright than the spots for the other APIM-containing proteins, and clear colocalization with PCNA was seen in only ∼20% of the S phase cells in comparison with 95–100% for hABH2, TFIIS-L, TFII-I, and Topo II α. This indicates that the PCNA–RAD51B interaction is less prominent and might require specific cell conditions.

In summary, the work presented in this study strongly indicates that APIM is a functional, widespread PCNA-interacting motif found in many proteins involved in genome maintenance. Among other interesting APIM-containing proteins are the poly(ADP-ribose) family (PARP-1, -2, and -4), the FANCC protein, the REV3L subunit of translesion polymerase ζ, several E3 ubiquitin protein ligases, subunits of the general transcription factors II and III, members of the MAPK pathway, many serine/threonine protein kinases, and three subunits of RNA polymerase II and III (Table I). Interestingly, recent data indicate a partial overlap between regions of replication and transcription (Malyavantham et al., 2008); thus, APIM could possibly be involved in linking transcription and cell cycle regulation to PCNA/replicative processes after genotoxic stress.

The scaffold protein PCNA interacts with numerous proteins in a well-orchestrated fashion, thus constituting a foundation for many vital cellular processes. Interactions with PCNA are likely to be regulated at several levels; e.g., by PTMs as well as through several PCNA-interacting motifs (Moldovan et al., 2007). Interestingly, PCNA-binding peptides containing the PIP box fused to GFP are reported to block colony formation when expressed in untreated freely cycling HeLa and U2OS cells (Warbrick, 2006). Cells expressing APIM-YFP had normal capacity for colony formation in untreated cells, but these cells showed increased sensitivity to alkylating agents. We suggest that impaired PCNA binding of several APIM-containing proteins, in addition to hABH2, contributes to the

are the result of three individual experiments (mean ± SEM; n = 35–50). (E) Cross-linked and reverse cross-linked IPs (α-Flag) from cells stably expressing hABH2$_{1–7}$YFP-Flag and hABH2$_{1–7}$F4A-YFP-Flag. The eluted fractions were analyzed for the presence of PCNA and Flag fusion proteins by WB. (F) 2D gel electrophoresis followed by WB analysis of PCNA immunoprecipitated from cross-linked hABH2$_{1–7}$-YFP-Flag (top membrane; α-Flag) and hABH2$_{1–7}$F4A-YFP-Flag (mid membrane; α-Flag). Total PCNA was immunoprecipitated with α-PCNA beads (lower membrane). Purified recombinant RAD51 (rRAD51) was added as an internal standard. Dotted lines illustrate the vertical alignment of the membranes. (B and E) Gray lines indicate that intervening lanes have been spliced out.

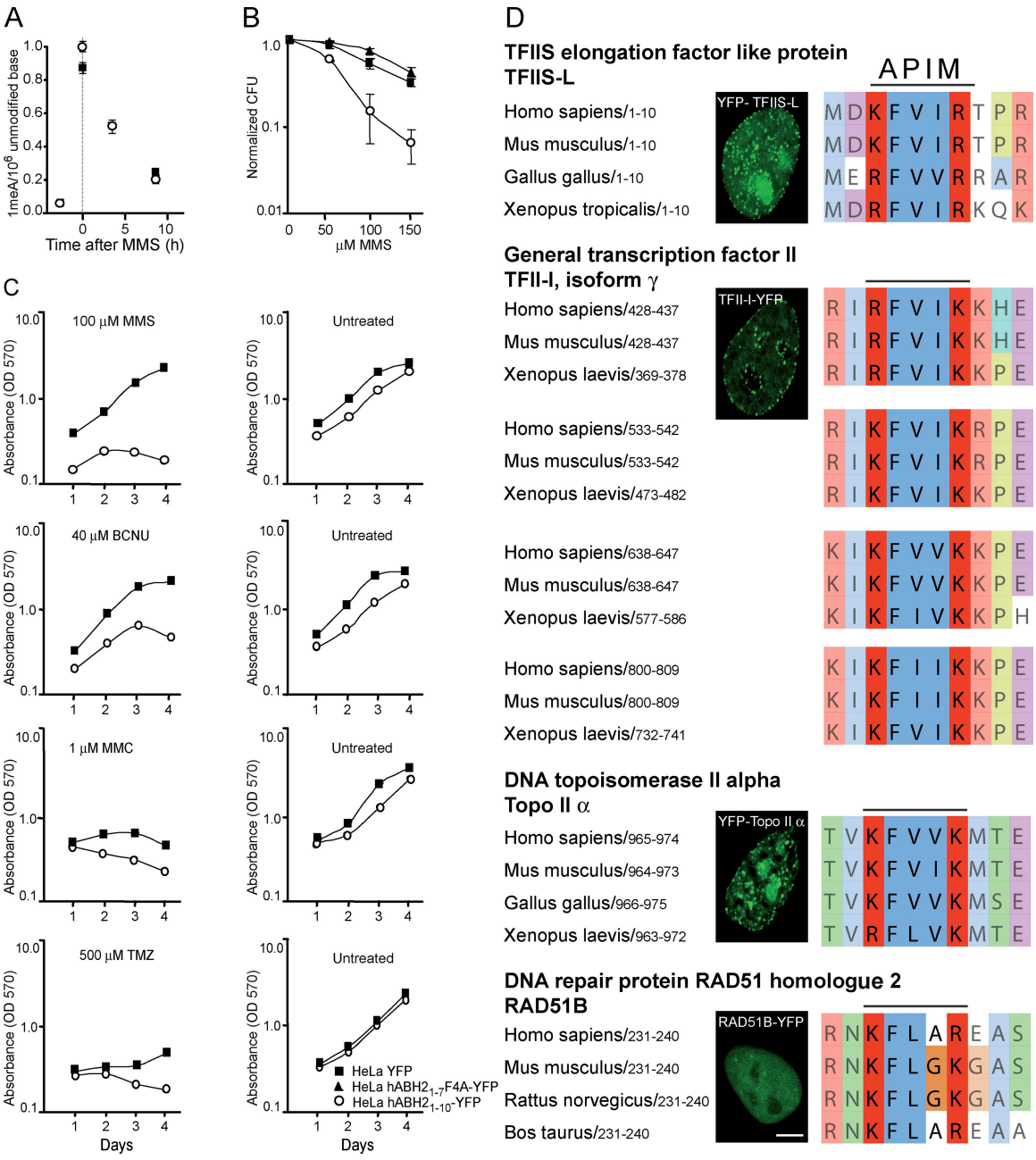

Figure 3. **Expression of APIM decapeptide sensitizes cells to alkylating agents, and several foci-forming proteins contain conserved APIM.** (A) 1meA in DNA isolated from YFP (closed squares)- and hABH2$_{1–10}$-YFP (open circles)–expressing cells after exposure to 1.2 mM MMS for 1 h before release from the G1/S border (mean ± SEM; n = 4–5). (B) Clonogenic assay comparing the MMS sensitivity between cells expressing hABH2$_{1–10}$-YFP (open circles), hABH2$_{1–7}$F4A-YFP (closed triangles), or only YFP (closed squares; mean ± SD; n = 2–4). CFU, colony-forming unit. (C) Cell growth of HeLa cells stably expressing YFP (closed squares) and hABH2$_{1–10}$-YFP (open circles) measured by MTT assay after continuous exposure to MMS, BCNU, MMC, and TMZ. The growth rates of unexposed cells are shown in the right lane. (D) Conservation of APIM in TFIIS-L, TFII-I, Topo II α, and RAD51B. These proteins are shown as YFP fusion proteins. Bar, 5 μm.

hypersensitivity to cytostatic drugs seen in APIM-expressing cells and that coordinated binding of APIM-containing proteins to PCNA might be an important response mechanism subsequent to DNA damage.

Materials and methods

Expression constructs

Cloning of the fluorescently tagged expression constructs CFP-PCNA, *Hereactis crispa* RFP (HcRed)–PCNA, and hABH2$_{1–261}$-YFP/-CFP has been described previously (Aas et al., 2003; Otterlei et al., 2006). Using phABH2$_{1–261}$-YFP as a template, phABH2$_{1–10}$-YFP and phABH2$_{11–261}$-YFP were generated by PCR and cloned into pYFP-N1 (Clontech Laboratories, Inc.) using NdeI–AgeI and AgeI–EcoRI, respectively. The PCR product from EST (image clone 5176979 [BC035374] Resource Center/Primary Database) was cloned into pYFP- and pCFP-C1 (HindIII–Acc651) to make pYFP- and pCFP–TFIIS-L. pTFII-I–YFP and –CFP were generated by PCR amplification of TFII-I from pI3CX–TFII-I (provided by R.G. Roeder, The Rockefeller University, New York, NY) and cloning into pYFP- and pCFP-N1 (SacI–ApaI). pYFP– and pCFP–Topo II α were made by switching the EGFP tag (EcoRI blunt–NheI) with YFP and CFP tag (XhoI blunt–NheI) from pEGFP–Topo II α (pT104-1; provided by

Table I. **Selected proteins containing APIM**

Type/group of proteins	Proteins	Source
Proteins containing PIP box and APIM	**DNA ligase I**, MDN1 Midasin, ubiquitin thioesterase FAF-X, protein 18 homologue (hVPS18), cytokine signaling 6 (SOCS-6), Topo II β, IκB-related protein, UHRF2, PARP4	Moldovan et al., 2007
DNA polymerase	**Pol ζ catalytic subunit** (hREV3L)	Moldovan et al., 2007
DNA ligases	**DNA ligase I**, DNA ligase IV	Moldovan et al., 2007
Topo	**Topo II** α and β	This study; Niimi et al., 2001; Lou et al., 2005
DNA repair proteins	**hABH2**, **PARP-1**, -2, and -4, **RAD51B**, **FANCC**, XPA	This study; Simbulan-Rosenthal et al., 1999; Jacquemont and Taniguchi, 2007
DNA repair–associated/ interacting proteins	XPA-binding protein 2, BRCA1/BRCA2-containing complex subunit 45 (prot-BRE), x-ray radiation resistance-associated protein 1	NA
Sister chromatid cohesion	***N*-acetyltransferase ESCO1/EFO1**, **hSMC5**	Potts et al., 2006; Moldovan et al., 2007
Chromatin remodelling and DNA-binding proteins	Chromodomain helicase DNA-binding proteins 3–5, p325 subunit of remodeling and spacing factor chromatin–remodelling complex, **telomeric repeat–binding protein 2 (TRF2)**	Opresko et al., 2004
E3 ubiquitin ligases	**UHFR1**, UHFR2, UBR1, UBR2, ring finger proteins 3, 17, and 151, probable E3 ubiquitin protein ligase MYCBP2	Bronner et al., 2007
Transcription factors	**TFIIS-L**, **TFII-I**, TFIIE-α, sterol regulatory element-binding transcription factor 2 (SREBF2), TFIIIC subunit α, TFIID 100 kD subunit (TAF5), TFIIIC 102 kD subunit (TF3C γ), transcription factor–like protein MRG15 and X (mortality factor 4–like proteins 1 and 2), E2 transcription factor 7	This study
Cell cycle regulators	Cell division cycle-associated 2, Bcl2-interacting mediator of cell death, testis spermatocyte apoptosis-related gene 2 protein	NA
Protein kinases	Serine/threonine (S/T) protein kinases SRPK1 and -2, 33 and MST4, leucine-rich repeat S/T protein kinase 1, STK23 (S/T protein kinase 23), S/T protein kinase PLK3, microtubuli-associated S/T protein kinase, microtubuli-associated S/T protein kinase 1, MAPKAP kinase 2 (MK2) and 5 (MK5), mitogen-activated protein kinase 15 (MSK-15)	NA
Methyltransferase	H3 lysine 4–specific MLL3, H3-K9 methyltransferase 5, putative rRNA methyltransferase 3	NA
Cancer-associated antigens	Melanoma-associated antigen E1 (MAGE E1), MAGE B18, MAGE-G1, natural killer tumor recognition protein (NK-TR), Myc-binding protein–associated protein, Myb-binding protein 1A, hepatoma-derived growth factor–related protein 2 isoform1, serologically defined colon cancer antigen 1	NA
RNA polymerase and ribosome-associated proteins	RNA polymerase II, largest subunit (RPB1), RNA polymerase III subunit 5 (RPC5), RNA polymerase II 140 kD (RPB2), UTP14A U3 small nucleolar RNA-associated protein 14 homologue A, 60S ribosomal protein L18, 60S ribosomal protein L35, TAF5-like RNA polymerase II p300 (PAF65-beta), mediator of RNA polymerase II transcription subunit 12 homologue	NA

NA, not applicable. Bold indicates proteins localized in replication foci under normal conditions or after DNA damage. The full lists of hits for the APIM and PIP motifs are available at http://tare.medisin.ntnu.no/pcna/index.php.

W.T. Beck, University of Illinois, Chicago, IL). RAD51B was amplified by PCR from pET15b-RAD51B (provided by S. Yokoyama, RIKEN Genomic Sciences Center, Kanagawa, Japan) and cloned into pYFP- and pCFP-N1 using XhoI and SacII. The hABH2$_{1-7}$-YFP constructs, including the F4 mutants, were made by annealing oligos with XhoI–EcoRI overhang followed by cloning into pYFP-N1 mutated in the ATG codon. The Flag constructs were generated by PCR amplification of the 3× Flag tag from p3×Flag–CMW-14 (Sigma-Aldrich) followed by cloning into pCFP-N1 in the BsrGI–XbaI site. All point mutations were made by site-directed mutagenesis (QuickChange II; Agilent Technologies) according to the manufacturer's instructions. Restriction enzymes and calf intestinal alkaline phosphatase were obtained from New England Biolabs, Inc., and the oligonucleotides were obtained from MedProbe Eurogentech. All constructs were verified by sequencing.

Confocal imaging

HeLa cells were examined 16–48 h after transient transfection (by Fugene 6 [Roche] or Lipofectamine 2000 [Invitrogen] according to the manufacturer's recommendations) of CFP, YFP, and HcRed fusion constructs. Fluorescent images were aquired using a laser-scanning microscope (LSM 510 Meta; Carl Zeiss, Inc.) equipped with a Plan Apochromat 63× 1.4 NA oil immersion objective. The images were acquired in the growth medium of the cell with the stage heated to 37°C using LSM 510 software (Carl Zeiss, Inc.). For the two-color images, CFP was excited at λ = 458 nm and detected at λ = 470–500 nm, and YFP was excited at λ = 514 nm and detected at λ = 530–600 nm using consecutive scans. When three-color images were acquired, YFP was excited at λ = 488 nm and detected at λ = 530–600 nm, HcRed was excited at λ = 543 nm and detected at λ > 560 nm, and the CFP settings were kept as for the

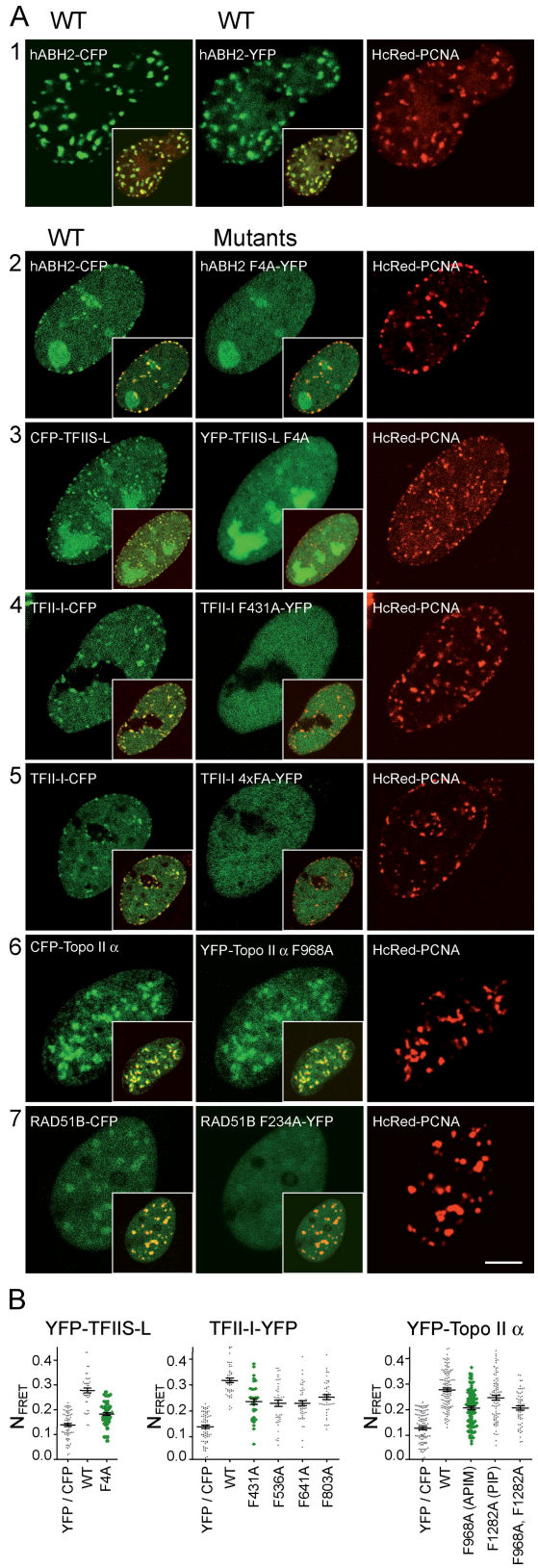

Figure 4. **Point mutations in APIM result in disrupted colocalization and reduced FRET.** (A) Row 1 shows confocal images of cotransfected WT hABH2-CFP, WT hABH2-YFP, and HcRed-PCNA. Rows 2–7 show confocal images of the WT proteins with CFP tag (left; green) cotransfected with YFP-tagged proteins mutated in APIM (middle; green), and HcRed-PCNA (right; red) in live cycling HeLa cells. Insets show merged images with PCNA. Bar, 5 µm. (B) N_{FRET} calculated for constructs in which single APIM mutation does not disrupt colocalization. WT and mutant proteins (YFP fusions of TFIIS-L, TFII-I, and Topo II α) are coexpressed with CFP-PCNA. YFP/CFP (vectors only) were used as background. Data are the results of two (TFIIS-L and TFII-I) to four (Topo II α) independent experiments. Error bars indicate mean ± SEM (n = 36–119).

two-color images. The thickness of the slice was 1 µm. No image processing, except contrast and intensity adjustments, were performed.

Immunofluorescence

HeLa cells were fixed in freshly made 2% paraformaldehyde on ice for 10 min before cold (−20°C) methanol was added, and the cells were incubated at −20°C for 20 min. All dilutions and washes were performed in 2% FCS in PBS. The cells were washed (three times for 5 min) before addition of 1 µg/ml α-PCNA (PC10; Abcam) and incubation for 1 h at 37°C. Finally, the cells were incubated for 1 h at 37°C with the secondary antibody Alexa Fluor 546 goat anti–mouse (diluted 1:2,000; Invitrogen). After washing, the cells were analyzed in a laser-scanning microscope (LSM 510 Meta; described in the previous paragraph), with excitation at 546 nm and detection >560 nm for goat anti–mouse and 488 nm excitation and detection between 505 and 550 nm for YFP, using consecutive scans.

FRET measurements

FRET occurs if the tags (YFP and CFP) are <100 Å (10 nm) apart (Mátyus, 1992). We detected FRET using the sensitized emission method, measuring acceptor (YFP) emission upon donor (CFP) excitation. FRET was scored when the intensity of emitted light from YFP after excitation of the CFP fluorochrome was stronger than the light emitted by CFP- or YFP-tagged proteins alone after excitation with the YFP and CFP lasers, respectively (bleed through), given by the equation $FRET = I_2 - I_1 (I_{D2}/I_{D1}) - I_3 (I_{A2}/I_{A3})$, in which I indicates mean intensities. YFP and CFP (vectors only) were used to measure background FRET because of dimerization of the tags, and YFP-PCNA and CFP-PCNA (because PCNA is a homotrimer) were used as positive control. FRET > 0 was normalized for expression levels using the equation $N_{FRET} = FRET/(I_1 \times I_3)^{1/2}$ (Mátyus, 1992; Xia and Liu, 2001; Otterlei et al., 2006). N_{FRET} was calculated from mean intensities within a region of interest containing >25 pixels in which all pixels had intensities <250, and the mean intensities were between 100 and 200. Channels 1 (CFP) and 3 (YFP) were measured as described for imaging, and channel 2 (FRET) was excited with λ = 458 nm and detected at λ = 530–600 nm. I_{D1-D3} and I_{A1-A3} were determined for cells transfected with CFP and YFP constructs only with the same settings and fluorescence intensities as cotransfected cells (I_1 and I_3).

Culture of cell lines and preparation of cell extracts

HeLa (cervical cancer) cells stably expressing the constructs of interest were prepared by transfection (Fugene 6) followed by cell sorting or cloning by dilution, and prolonged culturing in 400 µg/ml selective (using genticine; G418; Invitrogen) high glucose, 4.5 g/liter DME (BioWhittaker) supplemented with 10% FCS, 250 µg/ml amphotericin B (Sigma-Aldrich), 100 µg/ml gentamycin (Invitrogen), and 1 mM glutamine (BioWhittaker). The cells were cultured at 37°C in a 5% carbon dioxide–humidified atmosphere. Fractionated cell extracts from HeLa were prepared by resuspending the cell pellets in 1× packed cell volume (PCV) in buffer I (10 mM Tris-HCl, pH 8.0, and 50 mM KCl) and 1× PCV in buffer II (10 mM Tris-HCl, 100 mM KCl, 20% glycerol, 0.5% Nonidet P-40, 10 mM EGTA, 10 mM $MgCl_2$, 1 mM DTT, 1× complete protease inhibitor [Roche], and phosphatase inhibitor cocktail [PIC I and II; Sigma-Aldrich]). Cells were incubated under constant shaking for 30 min at 4°C, centrifuged at 2,000 rpm, and the supernatant (soluble fraction) was harvested. The pellet (containing nuclei) was resuspended in 1× PCV of buffer III (10 mM Tris-HCl, pH 8.0, and 100 mM KCl), 1× PCV buffer II, and sonicated. The sonicated nuclear pellet was incubated with 2 µl DNase/RNase cocktail I (200 U/µl Omnicleave Endonuclease; Epicentre Technologies), 1 µl DNase (10 U/µl; Roche), 1 µl bensonase (250 U/µl; EMD), 1 µl micrococcal nuclease (100–300 U/mg; Sigma-Aldrich), and 10 µl RNase (2 mg/ml; Sigma-Aldrich) per 30 mg cell extract at 37°C for 1 h. This fraction, denoted chromatin-enriched fraction, was dialyzed against buffer II and III followed by clearance by centrifugation before IP.

Formaldehyde cross-linking of proteins in intact cells
Cells were harvested and washed twice with cold PBS. 5–6 × 10^6 cells were resuspended in 10 ml PBS containing 0.25% formaldehyde and incubated at 37°C for 20 min. Cross-linking was stopped by adding glycine (final concentration 0.125 M). Cells were collected by centrifugation and washed once in PBS, resuspended in 8× PCV in buffer (20 mM Hepes, pH 7.9, 1.5 mM $MgCl_2$, 100 mM KCl, 0.2 mM EDTA, 20% glycerol, 0.5% NP-40, 1 mM DTT, and complete protease inhibitor) containing 5 µl Omnicleave, and sonicated. DNase/RNase cocktail I was added, and the homogenate was incubated at room temperature for 1 h and dialyzed at 4°C overnight in buffer (20 mM Hepes, pH 7.9, 1.5 mM $MgCl_2$, 100 mM KCl, 0.2 mM EDTA, 10% glycerol, 1 mM DTT, and complete protease inhibitor).

co-IP
An in-house affinity-purified rabbit polyclonal antibody raised against GFP protein, which also recognizes YFP and CFP proteins (called α-YFP), and monoclonal α-PCNA antibody (PC10; Santa Cruz Biotechnology, Inc.) were covalently linked to protein A paramagnetic beads (Invitrogen) according to instructions provided by New England Biolabs, Inc. 1,500 µg total cell–protein of the fractions was incubated with an additional 2 µl Omnicleave during IP with 10 µl antibody-coupled beads under constant rotation at 4°C over night (IP). The beads were washed four times with 200 µl 10 mM Tris-HCl and 50 mM KCl, pH 8, with a 5-min incubation on ice in between. The beads were resuspended in NuPAGE (Invitrogen) loading buffer and 1 mM DTT, heated, and the IP elutions were separated on 4–12% Bis-Tris-HCl (NuPAGE) gels. 50 µg cell extract was used for input.

IP of cross-linked protein extracts
Cross-linked Flag fusion proteins were immunoprecipitated using anti-Flag M2 affinity gel (herein referred to as α-Flag; Sigma-Aldrich) according to the manufacturer's protocol. The resin was prepared by washing once with 0.1 M glycine and 0.5 M NaCl, pH 3.0, and three times with TBS buffer (50 mM Tris HCl, pH 7.4, 150 mM NaCl, 10 mM Na butyrate, and 20 mM NaF). 2.5 mg and 5 mg (hABH2$_{1–7}$-YFP and hABH2$_{1–7}$F4A-YFP, respectively) of cross-linked extracts were incubated with 20 µl or 40 µl resin, respectively (packed gel volume), for 2 h at 4°C under constant rotation. The resin was washed three times with 500 µl of TBS buffer, and the cross-linked Flag fusion proteins were eluted by incubating the resin with 100 µl 3× Flag peptide in TBS buffer (final concentration of 450 ng/µl) for 30 min at 4°C under constant rotation. The cross-linking was reversed by a 30-min incubation at 95°C. For further WB analyses, the IP elution fractions were heated in 1× LDS sample buffer (NuPAGE) and 0.1 M DTT (65°C for 10 min) before loading 4–12% Bis-Tris-HCl (NuPAGE) gels.

2D gel electrophoresis
Immunoprecipitates of cross-linked extracts of hABH2$_{1–7}$YFP–3× Flag (5 mg) and hABH2$_{1–7}$F4A-YFP-3× Flag (10 mg) pulled down with α-Flag resin (40 µl and 80 µl, respectively) and by magnetic α-PCNA–coupled beads (50 µl beads; 2 mg extract) was subjected to 2D Western analysis. The resin was washed three times with 500 µl of TBS buffer. The resin was washed once in 20 mM Tris HCl, pH 7.4, 50 mM NaCl, 10 mM Na butyrate, and 20 mM NaF, and the cross-linked Flag fusion proteins were eluted by incubating the resin with 100 µl 3×Flag peptide in this buffer (final concentration of 450 ng/µl) for 30 min at 4°C under constant rotation. First dimension: after IP and elution, the cross-links were reversed (see previous paragraph), the α-PCNA beads were washed three times with 10 mM Tris-HCl and 50 mM KCl (1 ml), and resuspended in 340 µl destreak with 1% IPG buffer, pH 4–7 (GE Healthcare). After incubation overnight in a shaker at 4°C, the elutions were collected in separate vials without α-PCNA beads. 20 ng recombinant RAD51 protein (molecular mass, 37 kD; pI, 5.4; provided by I. Hickson Weatherall, University of Oxford, Oxford, England, UK) was added to each sample to serve as an internal standard. The samples were used to rehydrate immobiline DryStrips (18 cm; pH 4–7; GE Healthcare) overnight. The isoelectric focusing was performed according to the manufacturer's instructions in the IPGphor II unit (GE Healthcare). After isoelectric focusing, strips were cut after pH 5.5, and the pieces from pH 4–5.5 were incubated in equilibrium buffer (50 mM Tris-HCl, pH 8.8, 6 M urea, 30% glycerol, and 2% SDS) containing 1% DTT for 15 min followed by a 15-min incubation in the same buffer containing 2.5% iodoacetamide instead of DTT. Second dimension: the strips were loaded onto NuPAGE Novex 4–12% gels (Invitrogen).

WB
After gel electrophoresis, the polyvinylidene fluoride membranes (Immobilon; Millipore) were blocked in 5% low fat dry milk in PBST (PBS with 0.1% Tween 20). The primary antibodies, α-PCNA (PC10), α-hABH2 (monoclonal; Sigma-Aldrich), and α-Flag (monoclonal; Sigma-Aldrich), as well as the secondary antibodies, polyclonal rabbit anti–mouse IgG/HRP and polyclonal swine anti–rabbit IgG/HRP (Dako), were diluted in 1% dry milk in PBST. The membranes were treated with chemiluminescence reagent (SuperSignal West Femto Maximum; Thermo Fisher Scientific), and the proteins were visualized in Image Station (2000R; Kodak).

Dot blot analysis of predicted PCNA-binding peptides
An amino PEG500-UC540 sheet (acid hardened with improved stability) containing dots of 28 nmol peptide (stained with Ponceau to visualize the spots) was prepared at the peptide synthesis laboratory at The Biotechnology Center (University of Oslo, Oslo, Norway). The membrane was probed with 1 µg/ml PCNA for 2 h followed by probing with α-PCNA (PC10) and developed as described for WB. Data extracted from one representative dot blot is shown.

Sequence analysis
Details are provided at http://tare.medisin.ntnu.no/pcna/index.php.

MTT assay
HeLa cells stably expressing hABH2$_{1–10}$-YFP and YFP were seeded into 96-well plates (4,000 cells/well) and incubated for 3 h. Various doses of MMS (Acros Organics), BCNU (1,3-Bis(2-chloroethyl)-1-nitrosurea; Sigma-Aldrich), TMZ (4-methyl-5-oxo-2,3,4,6,8-pentazabicyclo [4.3.0] nona-2,7,9-triene-9-carboxamide; Sigma-Aldrich), and MMC (6-amino-1,1a,2,8,8a,8b-hexahydro-8-(hydroxymethyl)-8a-methoxy-5-methyl-azirino[2′,3′:3,4] pyrrolo[1,2-a]indole-4,7-dione carbamate; Sigma-Aldrich) were added to the wells. The cells were exposed continuously until harvest. MTT was added to the cells, the OD was measured at 570 nm, the mean from at least six wells was used to calculate cell survival, and the SD was smaller than the size of the dots. Data presented show growth from one representative experiment and has been reproduced at least two times.

Clonogenic assay
750 cells were seeded out in 10-cm cell culture dishes in 10 ml growth media and grown for 10 d. The cells were fixed in 6% glutaraldehyde in PBS for 15 min at room temperature, washed once in PBS, and stained with crystal violet, and colony-forming units were counted. Only colonies consisting of at least 50 cells were included. Data presented are mean ± SD from two (hABH2$_{1–7}$F4A-YFP) and four (hABH2$_{1–10}$-YFP and YFP) independent experiments.

Quantitation of 1meA in DNA
HeLa cells stably expressing hABH2$_{1–10}$-YFP and YFP were synchronized by the double thymidine block and analyzed by flow cytometry to verify the cell cycle phase. The DNA analysis of the cells was performed after methanol fixation (70%), RNase treatment (100 µg/ml in PBS at 37°C for 30 min), and propidium iodide staining (50 µg/ml in PBS at 37°C for 30 min) on an FACS flow cytometer (Canto; BD).

During G1/S arrest, the cells were treated with 1,200 µM MMS for 1 h, released, and harvested at defined time points. The cell pellets were washed with ice-cold PBS, spun down, snap frozen in liquid N_2, and stored at −80°C before use. DNA was isolated using DNeasy Blood and Tissue kit (QIAGEN). DNA samples were degraded enzymatically to deoxynucleosides and analyzed by LC/MS/MS using an HPLC system (Prominence; Shimadzu) interfaced with a triple-quadrupole mass spectrometer (API5000; Applied Biosystems), essentially as described previously (Ringvoll et al., 2006). 1meA and unmodified deoxynucleosides were monitored in multiple-reaction monitoring mode using the mass transitions 266.2→150.1 (1meA), 252.2→136.1 (deoxyadenosine), 243.2→127.1 (thymidine), 268.2→152.1 (deoxyguanosine), and 228.2→112.1 (deoxycytidine). Quantization was accomplished by comparison with pure deoxynucleoside standards.

We thank Drs. William T. Beck, Robert G. Roeder, and Shingeyuki Yokoyama for generously providing Topo II α, TFIH, and RAD51B constructs and Dr. Ian Hickson for providing purified RAD51.

This work is supported by The National Program for Research in Functional Genomics in Norway in The Research Council of Norway, The Cancer Fund at St. Olav's Hospital (Trondheim, Norway), The Norwegian Cancer Society, The Svanhild and Arne Must Fund for Medical Research (Norway), and the European Community (Integrated Project DNA repair; grant LSHG-CT-2005-512113).

Submitted: 25 March 2009
Accepted: 28 July 2009

References

Aas, P.A., M. Otterlei, P.O. Falnes, C.B. Vågbø, F. Skorpen, M. Akbari, O. Sundheim, M. Bjørås, G. Slupphaug, E. Seeberg, and H.E. Krokan. 2003. Human and bacterial oxidative demethylases repair alkylation damage in both RNA and DNA. *Nature.* 421:859–863.

Agostinho, M., J. Rino, J. Braga, F. Ferreira, S. Steffensen, and J. Ferreira. 2004. Human topoisomerase IIalpha: targeting to subchromosomal sites of activity during interphase and mitosis. *Mol. Biol. Cell.* 15:2388–2400.

Bronner, C., M. Achour, Y. Arima, T. Chataigneau, H. Saya, and V.B. Schini-Kerth. 2007. The UHRF family: oncogenes that are drugable targets for cancer therapy in the near future? *Pharmacol. Ther.* 115:419–434.

Cramer, P. 2004. RNA polymerase II structure: from core to functional complexes. *Curr. Opin. Genet. Dev.* 14:218–226.

Date, O., M. Katsura, M. Ishida, T. Yoshihara, A. Kinomura, T. Sueda, and K. Miyagawa. 2006. Haploinsufficiency of RAD51B causes centrosome fragmentation and aneuploidy in human cells. *Cancer Res.* 66:6018–6024.

Desgranges, Z.P., and A.L. Roy. 2006. TFII-I: connecting mitogenic signals to cell cycle regulation. *Cell Cycle.* 5:356–359.

Drabløs, F., E. Feyzi, P.A. Aas, C.B. Vaagbø, B. Kavli, M.S. Bratlie, J. Peña-Diaz, M. Otterlei, G. Slupphaug, and H.E. Krokan. 2004. Alkylation damage in DNA and RNA—repair mechanisms and medical significance. *DNA Repair (Amst.).* 3:1389–1407.

Fan, J., M. Otterlei, H.K. Wong, A.E. Tomkinson, and D.M. Wilson III. 2004. XRCC1 co-localizes and physically interacts with PCNA. *Nucleic Acids Res.* 32:2193–2201.

Helleday, T., E. Petermann, C. Lundin, B. Hodgson, and R.A. Sharma. 2008. DNA repair pathways as targets for cancer therapy. *Nat. Rev. Cancer.* 8:193–204.

Jacquemont, C., and T. Taniguchi. 2007. The Fanconi anemia pathway and ubiquitin. *BMC Biochem.* 8:S10.

Lehmann, A.R., A. Niimi, T. Ogi, S. Brown, S. Sabbioneda, J.F. Wing, P.L. Kannouche, and C.M. Green. 2007. Translesion synthesis: Y-family polymerases and the polymerase switch. *DNA Repair (Amst.).* 6:891–899.

Leonhardt, H., H.P. Rahn, P. Weinzierl, A. Sporbert, T. Cremer, D. Zink, and M.C. Cardoso. 2000. Dynamics of DNA replication factories in living cells. *J. Cell Biol.* 149:271–280.

Lou, Z., K. Minter-Dykhouse, and J. Chen. 2005. BRCA1 participates in DNA decatenation. *Nat. Struct. Mol. Biol.* 12:589–593.

Malyavantham, K.S., S. Bhattacharya, W.D. Alonso, R. Acharya, and R. Berezney. 2008. Spatio-temporal dynamics of replication and transcription sites in the mammalian cell nucleus. *Chromosoma.* 117:553–567.

Mátyus, L. 1992. Fluorescence resonance energy transfer measurements on cell surfaces. A spectroscopic tool for determining protein interactions. *J. Photochem. Photobiol. B.* 12:323–337.

Moldovan, G.L., B. Pfander, and S. Jentsch. 2007. PCNA, the maestro of the replication fork. *Cell.* 129:665–679.

Naryzhny, S.N. 2008. Proliferating cell nuclear antigen: a proteomics view. *Cell. Mol. Life Sci.* 65:3789–3808.

Nettikadan, S.R., C.S. Furbee, M.T. Muller, and K. Takeyasu. 1998. Molecular structure of human topoisomerase II alpha revealed by atomic force microscopy. *J. Electron Microsc. (Tokyo).* 47:671–674.

Niimi, A., N. Suka, M. Harata, A. Kikuchi, and S. Mizuno. 2001. Co-localization of chicken DNA topoisomerase IIalpha, but not beta, with sites of DNA replication and possible involvement of a C-terminal region of alpha through its binding to PCNA. *Chromosoma.* 110:102–114.

Opresko, P.L., M. Otterlei, J. Graakjaer, P. Bruheim, L. Dawut, S. Kølvraa, A. May, M.M. Seidman, and V.A. Bohr. 2004. The Werner syndrome helicase and exonuclease cooperate to resolve telomeric D loops in a manner regulated by TRF1 and TRF2. *Mol. Cell.* 14:763–774.

Otterlei, M., P. Bruheim, B. Ahn, W. Bussen, P. Karmakar, K. Baynton, and V.A. Bohr. 2006. Werner syndrome protein participates in a complex with RAD51, RAD54, RAD54B and ATR in response to ICL-induced replication arrest. *J. Cell Sci.* 119:5137–5146.

Potts, P.R., M.H. Porteus, and H. Yu. 2006. Human SMC5/6 complex promotes sister chromatid homologous recombination by recruiting the SMC1/3 cohesin complex to double-strand breaks. *EMBO J.* 25:3377–3388.

Ringvoll, J., L.M. Nordstrand, C.B. Vågbø, V. Talstad, K. Reite, P.A. Aas, K.H. Lauritzen, N.B. Liabakk, A. Bjørk, R.W. Doughty, et al. 2006. Repair deficient mice reveal mABH2 as the primary oxidative demethylase for repairing 1meA and 3meC lesions in DNA. *EMBO J.* 25:2189–2198.

Sedgwick, B., P.A. Bates, J. Paik, S.C. Jacobs, and T. Lindahl. 2007. Repair of alkylated DNA: recent advances. *DNA Repair (Amst.).* 6:429–442.

Simbulan-Rosenthal, C.M., D.S. Rosenthal, S. Iyer, H. Boulares, and M.E. Smulson. 1999. Involvement of PARP and poly(ADP-ribosyl)ation in the early stages of apoptosis and DNA replication. *Mol. Cell. Biochem.* 193:137–148.

Vasilescu, J., X. Guo, and J. Kast. 2004. Identification of protein-protein interactions using in vivo cross-linking and mass spectrometry. *Proteomics.* 4:3845–3854.

Warbrick, E. 2000. The puzzle of PCNA's many partners. *Bioessays.* 22:997–1006.

Warbrick, E. 2006. A functional analysis of PCNA-binding peptides derived from protein sequence, interaction screening and rational design. *Oncogene.* 25:2850–2859.

Xia, Z., and Y. Liu. 2001. Reliable and global measurement of fluorescence resonance energy transfer using fluorescence microscopes. *Biophys. J.* 81:2395–2402.

Xia, L., L. Zheng, H.W. Lee, S.E. Bates, L. Federico, B. Shen, and T.R. O'Connor. 2005. Human 3-methyladenine-DNA glycosylase: effect of sequence context on excision, association with PCNA, and stimulation by AP endonuclease. *J. Mol. Biol.* 346:1259–1274.